Spectrochimica Acta Part A: Molecular and Biomolecular Spectroscopy 211 (2019) 348–355

Contents lists available at ScienceDirect

Spectrochimica Acta Part A: Molecular and Biomolecular Spectroscopy

journal homepage: www.elsevier.com/locate/saa

Aqueous dispersible green luminescent yttrium oxide:terbium microspheres with nanosilica shell coating

Anees A. Ansari [a,*], Naushad Ahmad [b], Joselito P. Labis [a], Ahmed Mohamed El-Toni [a], Aslam Khan [a]

[a] King Abdullah Institute for Nanotechnology, King Saud University, Riyadh 11451, Saudi Arabia
[b] Department of Chemistry, College of Sciences, King Saud University, Riyadh 11451, Saudi Arabia

ARTICLE INFO

Article history:
Received 27 September 2018
Received in revised form 3 December 2018
Accepted 8 December 2018
Available online 11 December 2018

Keywords:
Y_2O_3:Tb
Microspheres
Zeta potential
Surface chemistry
Photoluminescence

ABSTRACT

Tb-doped Y_2O_3 microspheres (MSs) were prepared via a homogeneous thermal degradation process at a low temperature and then coated with a nanosilica shell (Y_2O_3:Tb@SiO_2) using a sol-gel process. The core MSs were highly crystalline and spherical with a porous surface, single cubic phase, and particle size of 100–250 nm. Transmission electron microscopy (TEM) images clearly showed the spherical shape of the as-prepared core MSs, which were fully covered with a thick and mesoporous nanosilica shell. Fourier transform infrared (FTIR) spectra displayed the well-resolved infrared absorption peaks of silica (Si—O, Si—O—Si, etc.), confirming the presence of the silica surface coating. The core MSs retained their spherical shape even after heat treatment and subsequent silica surface coating. It was observed that the core/shell MSs are easily dispersible in aqueous media and form a semi-transparent colloidal solution. Ultraviolet/visible and zeta potential studies were tested to prove the changes in the surface chemistry of the as-designed core/shell MSs and compare with their core counterpart. The growth of the amorphous silica shell not only increased the particle size but also enhanced remarkably the solubility and colloidal stability of the MSs in aqueous media. The strongest emission lines originating from the characteristic intra-shell 4f-4f electronic transitions of Tb ions were quenched after silica layer deposition, but the MSs still showed strong green ($^5D_4 \rightarrow {}^7F_5$ at 530–560 nm as most dominant) emission efficiency, which indicates great potential in fluorescent bio-probes. The emission intensity is discussed in relation to the quenching mechanism induced by surface silanol (Si-OH) groups, particle size, and surface charge.

1. Introduction

In recent years, the synthesis of luminescent lanthanide nano/micromaterials with controlled shape and size morphologies has opened new opportunities in photonic-based biomedical sciences [1–4]. Currently, the synthesis of preferably spherical luminescent nano/micromaterials represents an especially fascinating research field compared to the syntheses of those with other morphological structures and geometric features [5–10]. Compared to other one- and two-dimensional nano/micromaterials, spherical luminescent materials have distinctive features such as a high specific surface area, active surface sites, ionic intercalation, a porous surface, and low active densities, and they have prospective scale-dependent photonic-based biomedical applications [3,6,7,11–15]. The ideal morphology for a luminescent material includes a spherical shape, a narrow size distribution, and the absence of aggregation [6–10,12]. To date, many synthesis methods have been established for controlling the morphological structures and dispersibility of luminescent nano/micromaterials, including thermal decomposition, hydrothermal/solvothermal methods, polyol methods, combustion [16], the Pechini sol-gel method, and precipitation techniques [6–11,14,15,17–19]. Generally, urea was used as a weak base for the synthesis of luminescent nano/micro-materials through thermal decomposition technique at a low temperature [5–9,11,20]. The advantages of this method is that it involves lower-temperature synthesis, is economical and eco-friendly, and offers easy control of the morphology of the final luminescent nano/microspheres, which are weakly hydrophilic in nature because of the use of aqueous media. Among the luminescent lanthanide nano/micromaterials, Y_2O_3 is considered to be one of the most attractive phosphors because of its outstanding chemical and optical properties as a host lattice [2,3], such as high thermal conductivity and expansion coefficient, broad transparent range of 0.23–8 μm, and relatively low phonon energy (max. 600 cm^{-1}) [21,22]. Sotiriou et al. fabricated uncontrolled silica-coated Y_2O_3:Tb nanoparticles using a flame spray pyrolysis reactor [2,23,24]. Wu et al. applied a sol-gel technique for the synthesis of Y_2O_3:Tb nanoparticles [25], and a similar process was utilized by various researchers for their synthesis to investigate their optical properties [26–28]. Xu et al. used a polystyrene template for the preparation of uniform terbium-doped yttrium oxide hollow microspheres [5]. In another study, a co-precipitation method was employed for the synthesis of spherical microspheres [29–31].

* Corresponding author.
E-mail addresses: amustaqeemahmad@ksu.edu.sa, aneesaansari@gmail.com (A.A. Ansari).

https://doi.org/10.1016/j.saa.2018.12.015
1386-1425/

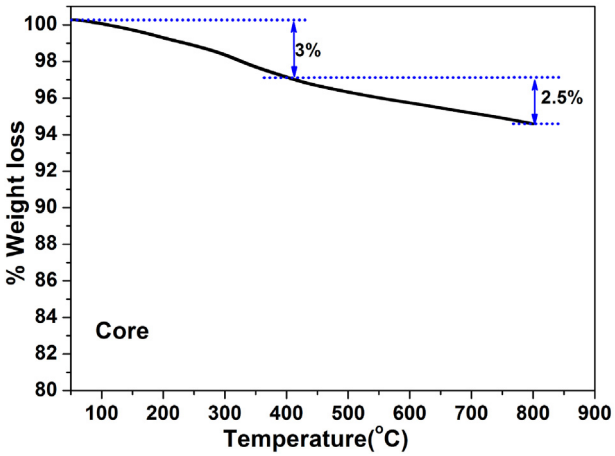

Fig. 1. Thermogravimetric analysis of core MSs.

Mukherjee et al. applied a combustion process for the preparation of Y_2O_3:Tb nano/microphosphors at a high temperature [32,33]. Most of the processes used result in uncontrolled growth of particles and are hydrophobic in nature. Because of the uncontrolled size of the nano/microphosphors, good luminescence efficiency was not achieved even under ambient conditions. It is well known that a controlled morphology with a designed crystal structure strongly affects the luminescence properties of particles. Therefore, their use in the biological window for the detection or labeling of bio-macromolecules is very limited. In the present study, we developed a facile urea-based homogeneous thermal decomposition process for the large-scale preparation of spherical and porous Y_2O_3 nano/microphosphors with high photoluminescence efficiency. The porous surface of the luminescent materials is highly desirable for tagging and labeling bio-macromolecules. Furthermore, the benefit of this method is that it is an inexpensive, eco-friendly, simple, low-temperature synthesis method that can easily afford spherical, hydrophilic, porous nano/microphosphors. More importantly, the preparation of luminescent nano/microphosphors, preferably spherical, is of concern because they offer the opportunity for higher photoluminescence performance, high definition, and more enhanced screen packing.

In order to improve the performance of luminescent nano/microspheres in the biological window, several efforts have been made to change the nano/microparticles from hydrophobic to hydrophilic through surface hydroxylation using silica or polymeric materials. Among the surface hydroxylation processes, coating with an amorphous silica surface has gained much attention owing to some attractive features such as high solubility in most polar solvents, transparency in the visible region, a stable mesoporous structure, eco-friendliness, low cost, excellent biocompatibility, and non-toxicity in nature [26,34–44]. Additionally, the silica layer has a tunable pore size distribution, offers easy surface alteration, and has an exceptionally large specific surface area with plentiful silanol (Si—OH) groups. These surface-modifying functional groups can bind easily with suitable bio-macromolecules through their functional groups (—OH, —NH_2, or —COOH) for loading and releasing drug molecules via an additional reproducible and predictable method. Because of their good fluorescence, solubility, colloidal stability, biocompatibility, and non-toxicity, silica-modified nano/microparticles have been considered for use in photonic-based applications in biological sciences [15,37,41,45–48]. Here, we present the synthesis of luminescent core microspheres (MSs) and silica-coated core/shell MSs and their characterizations with various physicochemical techniques such as transmission electron microscopy (TEM), energy dispersive X-ray (EDX) analysis, X-ray diffraction (XRD), Fourier transform infrared (FTIR) spectroscopy, FT-Raman spectroscopy, thermogravimetric analysis (TGA), dynamic light scattering (DLS), zeta potential measurement, and photoluminescence spectroscopy to examine the phase purity, particle size, morphological structure, thermal stability, surface chemistry, hydrophilicity, and optical and luminescence properties. The effects of amorphous silica layer deposition on the physicochemical and photoluminescence properties were studied, and these properties were compared with those of bare luminescent core MSs. In the core/shell structure, the silica layer interacts with the luminescent Y_2O_3:Tb (core) MSs, which affects the luminescence properties of the core/shell MSs. Most importantly, the as-designed MSs displayed strong green luminescence even after silica surface modification and good dispersibility in aqueous media.

2. Experimental Section

2.1. Materials

Y_2O_3 (99.9%, BDH Chemicals, UK), terbium oxide (99.99%, Alfa Aesar, Germany), tetraethyl orthosilicate (TEOS), NH_4OH, HNO_3, urea, and ethanol were used directly without further purification. Hydrated yttrium nitrate and terbium nitrates were synthesized by dissolving the corresponding metal oxides in dilute (0.01 M) HNO_3. Milli-Q (Millipore, Bedford, USA) water was used for the synthesis and characterization of the powder products.

2.2. Synthesis of Y_2O_3:Tb and Y_2O_3:Tb@SiO_2 Core/Shell MSs

In a typical synthesis of Y_2O_3:Tb MSs, a freshly prepared 0.2 M solution of yttrium nitrate ($Y(NO_3)_3 \cdot 6H_2O$, 3.895 g) and terbium nitrate ($Tb(NO_3)_3 \cdot 6H_2O$, 0.226 g, 1.25 mL) were added to 50 mL of distilled H_2O and the mixture was kept on a hot plate for mechanical stirring. Afterwards, 11 g of aqueous dissolved urea was introduced into the vigorously stirred solution to form a homogeneous mixture [6,8,11]. For the thermal decomposition of urea, the mixture was decomposed under reflux conditions at 150 °C for 3–4 h under constant magnetic stirring. The resulting precipitate was separated from the mixture by centrifugation and washed with distilled H_2O to remove unreacted reactants and then dried in a furnace at 600 °C for characterization [1,3,6,8,11,49,50].

A modified Stober method was employed to apply a silica surface coating over the luminescent MSs. With the help of ultrasonication, 500 mg of the as-synthesized Y_2O_3:Tb MSs were dispersed in a minimal amount of aqueous media [45,51,52]. Afterwards, the ultrasonicated MSs were centrifuged and re-dispersed in a solution of 150 mL of ethyl alcohol, 50 mL of distilled water, and 4 mL of ammonium hydroxide. The resulting solution was kept on a hot plate at ambient

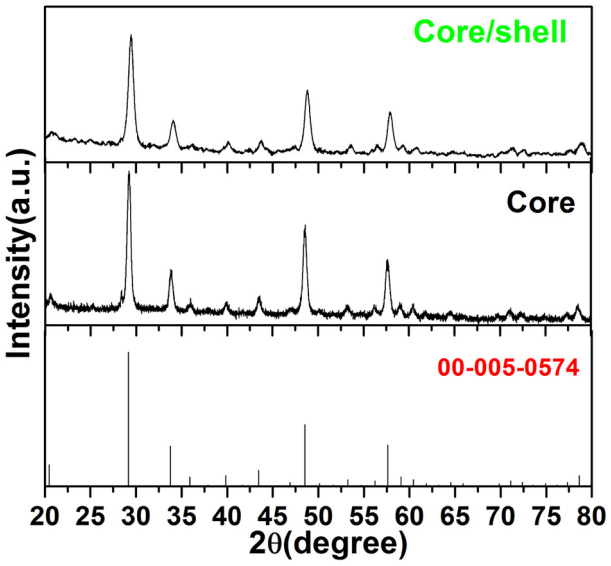

Fig. 2. X-ray diffraction pattern of core and core/shell MSs.

temperature for mechanical stirring. After 30 min, 1 mL of TEOS was added slowly into the strongly stirred solution and reaction proceeds for 5–6 h. The obtained product was separated from the mixture by centrifugation, washed with distilled H_2O, and dried overnight at 60 °C.

2.3. Characterization

The compositions and crystallinities of the products were examined using XRD with a PANalytical X'Pert X-ray diffractometer equipped with a Ni filter using Cu Kα (λ = 1.5406 Å) radiation. The morphologies were examined using a field emission-transmission electron microscopy (FE-TEM, JEM-2100F, JEOL, Japan) instrument functioning at an accelerating voltage of 200 keV. The TEM instrument was equipped for EDX, which was employed for elemental analysis. Water-suspended core and core/shell samples were used to measure the size distributions and zeta potentials using a Zeta PALS 90 plus particle size analyzer (Brookhaven Instruments Corp., Holtsville, NY, USA). TGA was conducted using a TGA/DTA instrument (Mettler Toledo AG, Analytical CH-8603, Schwerzenbach, Switzerland). Infrared spectra were obtained using a Vertex 80 (Bruker, USA) infrared spectrometer with the KBr pellet technique. Photoluminescence and Raman spectra were obtained using a 325 He-Cd laser (Jobin Yvon Horiba HR800 spectrophotometer). A slit width of 100 μm was used, ensuring a spectral resolution better than 1 cm^{-1} [47].

3. Results and Discussion

Fig. 1 shows the results of TGA with a heating rate of 10 °C/min of the as-synthesized materials, revealing the phase purity and thermal stability of the luminescent nanomaterials under a N_2 atmosphere. The initial weight loss (~3%) in the core sample was observed below 400 °C, which could be due to the loss of chemisorbed water and the loss of organic moieties that are trapped inside the pores. The second stage sluggish weight loss of approximately 2.4% was observed between 400 and 800 °C may be attributed to the presence of little carbonates which may be originated from air. Our results are in agreement with previous literature reports [5,53,54].

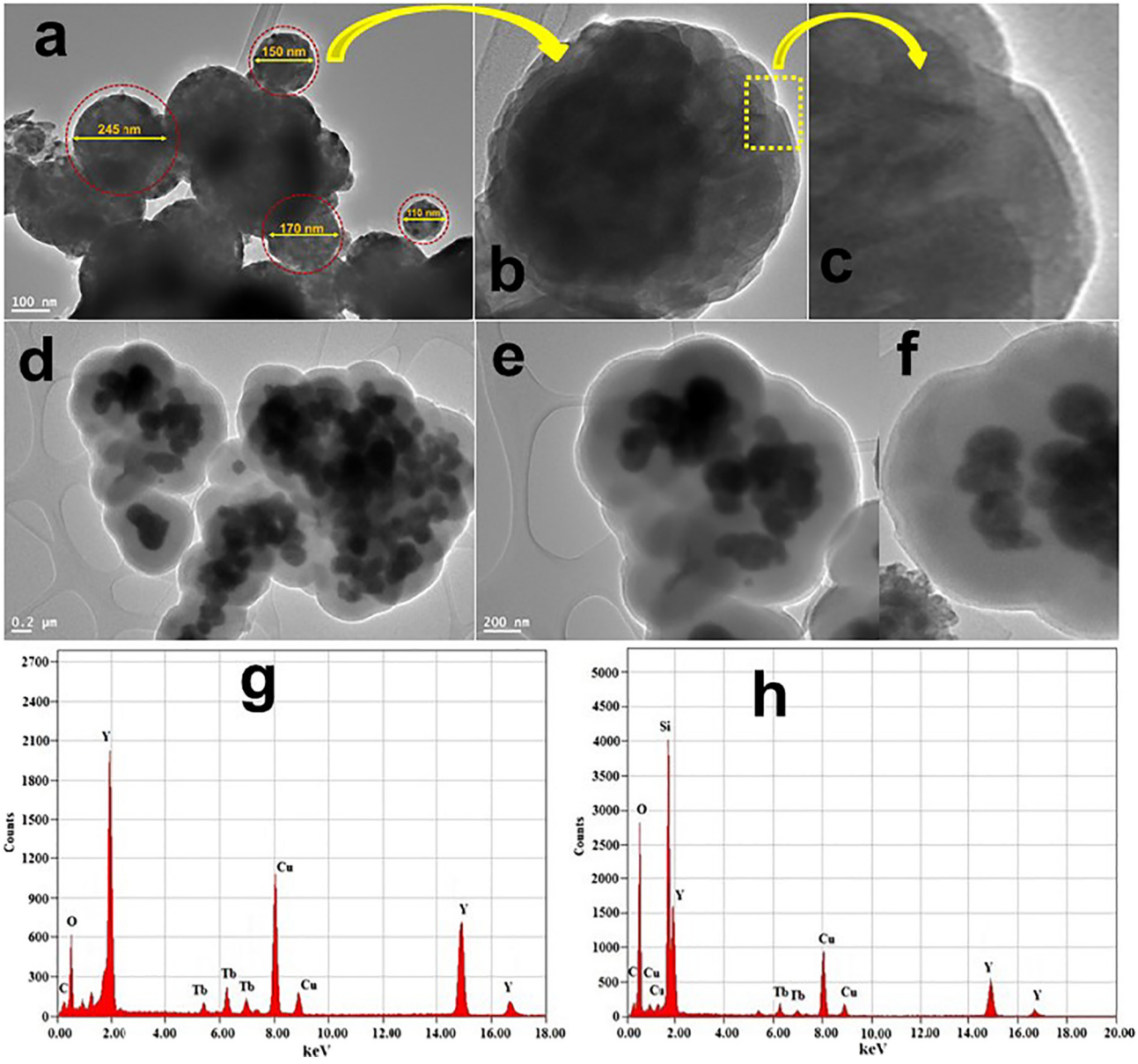

Fig. 3. TEM images of (a) low magnification core (b & c) single particle of core-MSs with high magnified rough surface (d) low magnification TEM image of core/shell (e) high resolution TEM image of core/shell (f) high magnification TEM image of core/shell (g) EDX spectrum of core (h) EDX spectrum of core/shell MSs.

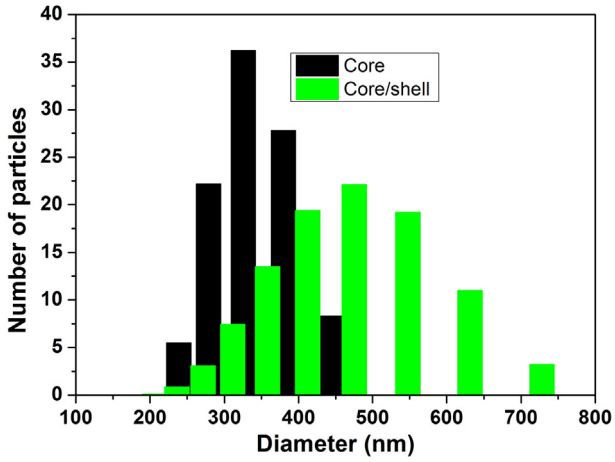

Fig. 4. Particle size distribution of core and core/shell MSs in aqueous media deduced in dynamic light scattering.

The powder XRD pattern was obtained to examine the compositions and crystallographic structures of the as-synthesized samples. All reflections in both samples corresponded well with the body-centered cubic Y_2O_3 phase (JCPDS No. 005-0574) [55]. As shown in Fig. 2, the peak locations and intensities matched with those in published literature reports [23,55]. The absence of any additional reflection peaks related to impurities or the amorphous form confirmed the composition and the successful homogeneous distribution of Tb^{3+} ions in the crystal matrix. As shown in Fig. 2, the amorphous silica surface coating did not altered the crystalline structure of the as-designed phosphor, because all diffraction planes in XRD pattern of core and core/shell MSs are almost identical in shape, position, and intensity [23]. However, the reflection peak intensity is slightly lower with a higher peak width for the core/shell sample because of the influence of the amorphous silica [56,57]. This indicated that the amorphous silica framework expanded the nanopore structure over the surface of the luminescent core MSs and rearranged the Si—O—Si network structure while containing no impurities.

The morphological structure and silica surface coating were examined through TEM images. The TEM images in Fig. 3a–b show the porous surface and reveal that the particles are irregular in size but spherical and highly aggregated with an average size of 100–250 nm. Previously our and some other research groups have reported that silica coating not only enhances the hydrophilicity but also improves the biocompatibility and non-toxicity of the lanthanide nanoparticles. [1,15,36,45,46,58–60]. No change in the morphological structure was observed after silica surface coating and the spherical shape was retained, but the particle size was larger than that of the corresponding non-silica-coated luminescent core MSs, owing to the growth of an additional amorphous silica layer (Fig. 3d–e). As shown in Fig. 3e–f, a mesoporous silica layer approximately 40–50 nm thick effectively covered the surface of the luminescent core MSs. Silica-coated MSs still aggregate in aqueous media because of the existence of abundant surface-bound hydroxyl groups, which are connected to each other through hydrogen bonding [15,59]. Additionally, the surface of silica-modified MSs is irregular, aggregated, and mesoporous, suggesting that the MSs are coated with silica via a sol-gel process. As shown in

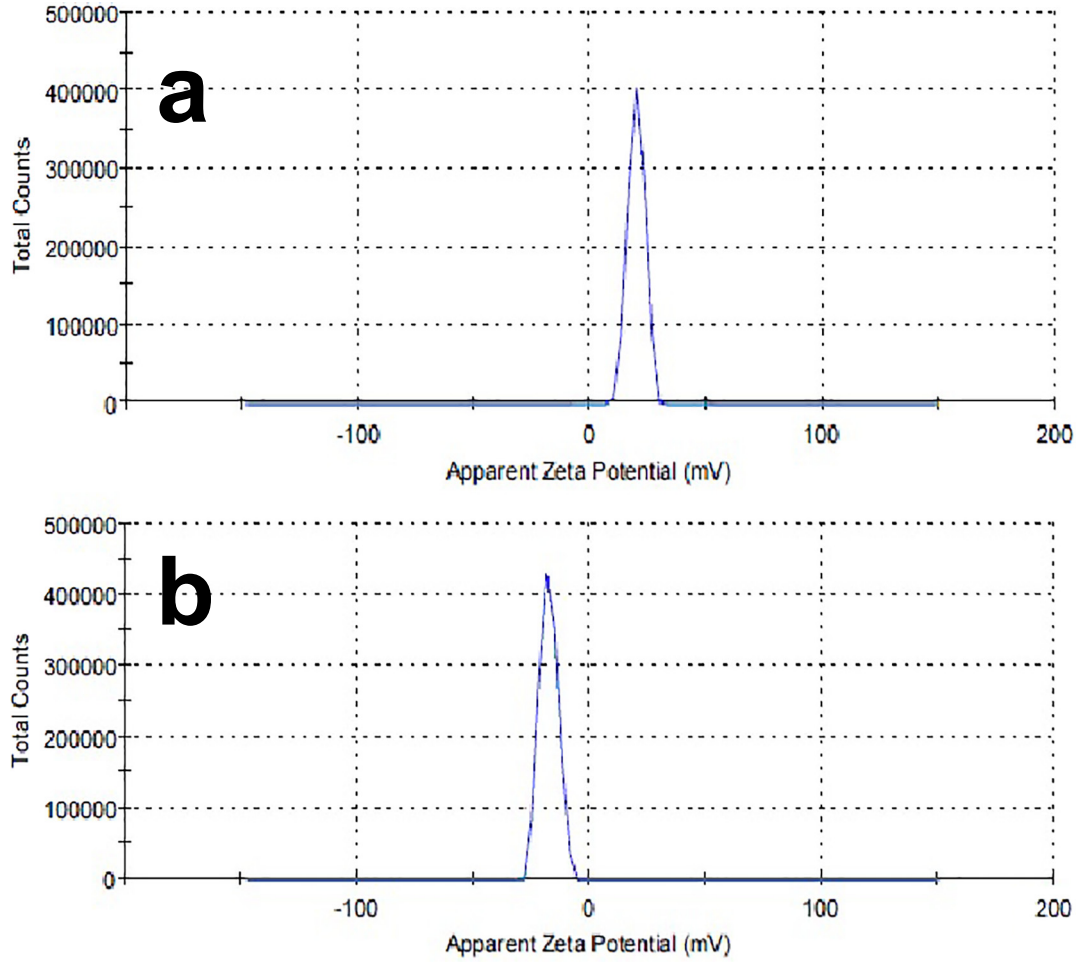

Fig. 5. Zeta potential graphs of (a) core and (b) core/shell MSs at physiological pH value.

Fig. 3d & f, the silica coating can be distinguished simply through dissimilar electron penetrability; the core is gloomy, black, and spherical and the silica layer is a mesoporous surface with a light grey color. Elemental analysis was carried out using EDX to verify the success of SiO_2 surface coating and the presence of doping constituents (Fig. 3g–h). As shown in Fig. 3g–h, all elements, namely Y, Tb, O, and Si, in the Y_2O_3:Tb and Y_2O_3:Tb@SiO_2 MSs appear in the spectrum, and the presence of the Si peak at approximately 1.68 keV (Fig. 3h) confirmed the successful application of an amorphous SiO_2 external coating over the luminescent core MSs. The appearances of the dominant C and Cu peaks were attributed to the carbon-coated copper grid.

DLS measurements were performed in aqueous media (pH = 7.0) to investigate the hydrodynamic size, surface charge, and biocompatibility of the as-synthesized core and core/shell MSs. At physiological pH, the average particle sizes of the as-synthesized core and core/shell MSs are 150–400 and 250–600 nm, respectively (Fig. 4). As shown in Fig. 4, the sizes of the core and core/shell MSs are larger than those from the TEM results. This was probably because the thick amorphous silica shells spread out and tend to form aggregates in aqueous media, which is consistent with the TEM image (Fig. 3a, c, & d). It is obvious from the TEM images that after the growth of the amorphous silica shell, the particles tended to increase in size. The observed zeta potential values at physiological pH were 19.7 and −17.6 mV for the core and core/shell MSs, respectively (Fig. 5). A remarkable difference in zeta potential values was observed after silica surface modification, revealing that the silica shell has a large number of hydroxyl groups, owing to the deprotonation value of silica-modified MSs (−17.6), which are more easily available for bonding with bio-macromolecules [61–63]. On increasing the pH value from 7 to 10, the zeta potential value decreased greatly from +19.7 to −21.2 mV for core MSs and from −17.6 to −68.2 mV for core/shell MSs (see Supplementary data). This indicates that high-surface-area core/shell MSs have good stability over a broad range of pH values.

The FTIR spectra show a characteristic strong infrared absorption band with doublet intensity located at 1090 cm^{-1} along with comparatively weak-intensity peaks located at 800 and 600 cm^{-1} ascribed to the stretching and bending vibrational modes of Si—O—Si, Si—O, and Si—OH, respectively (Fig. 6) [52,64–68]. The broad band at 3000–3700 cm^{-1} and two weaker-intensity peaks located at 800 and 600 cm^{-1} are attributed to the stretching, bending, and wagging vibrational modes of surface-adsorbed water and silanol groups [45,46,68]. A sharp infrared peak at 463 cm^{-1} corresponds to the metal-oxygen ν(M—O) vibration (Fig. 6) [45–47]. Raman spectroscopy was carried out to examine the structural disorder in the as-synthesized samples at room temperature. The Raman spectra of the core and core/shell MSs in Fig. 7 display all of the characteristic vibrational modes of the body-centered cubic structure of yttrium oxide located at 376, 469, and 637 cm^{-1}, which is in good agreement with previous observations [69,70]. In addition, the Raman peaks are intense and sharp, indicating strong interaction between the metal and oxygen ions in the sample. Furthermore, Raman spectroscopy verified the crystal structure of the materials, which was not altered even after the application of the amorphous silica surface coating. However, the Raman spectrum after coating with silica showed reduced intensity, which could be the result of the influence of amorphous silica surface modification. The absorption spectrum of the core/shell sample was measured in aqueous media to examine the solubility and colloidal immovability characteristics of the as-prepared sample (see Supplementary materials).

Photoluminescence spectra were measured to investigate the doping of luminescent terbium ions into the Y_2O_3 crystal matrix and the coating of the luminescent core MSs with mesoporous silica. The emission spectra were recorded at room temperature between 450 and 700 nm spectral range under monitoring at an excitation wavelength of 325 nm (3.82 eV) in aqueous media as well as solid phase, which corresponds to the $^5D_4 \rightarrow {}^7F_J$ transitions (where $J = 6, 5, 4, 3, 2$, etc.), and detection in the 450–700 nm range [24,34,47,51]. The

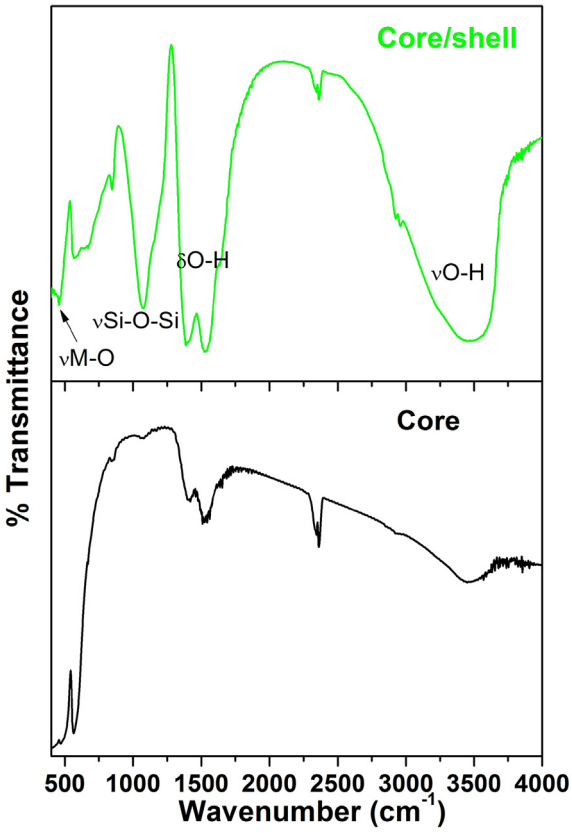

Fig. 6. FTIR spectra of the core and core/shell MSs.

photoluminescence spectra of both samples were measured in the solid phase with equal weights, and exhibited several strong and weak emission transitions in the visible region with multiple splittings (Fig. 8). The most prominent emission transition was observed in the middle of the visible region at 530–560 nm and was due to the so-called hypersensitive $^5D_4 \rightarrow {}^7F_5$ strongest green emission transition [28,34,47,51,71]. Notably, the emission transitions are highly suppressed for the core/shell MSs, despite the luminescent core sample, suggesting the successful application of the amorphous silica surface coating, which enhanced the multiphoton relaxation pathways, resulting in the quenched luminescence intensities of the transitions [36,40,65,72,73]. The absence of $^5D_3 \rightarrow {}^7F_j$ transitions in this work is

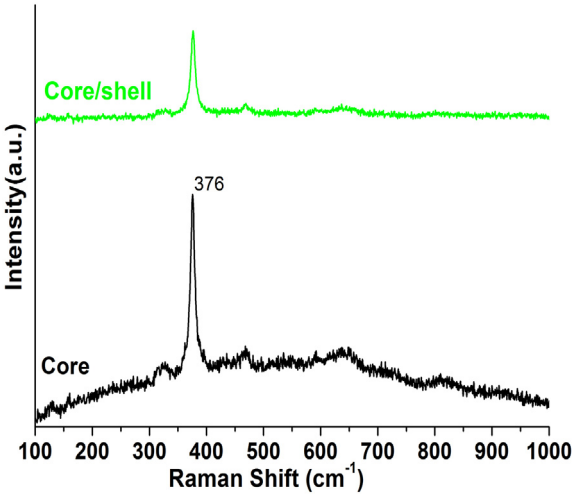

Fig. 7. FT-Raman spectra of the core and core/shell MSs.

related to increased doping concentration, which induces non-radiative de-excitation through cross relaxation [25]. As observed in Fig. 8e, the emission spectra in aqueous media shows similar pattern as measured in solid phase. No significant changes of emission spectra were observed in aqueous phase. The emission spectra in solid phase revealed multiple splitting; it could be due to higher values of *J*, which in turn split the levels into various sub-levels [51,74,75]. We expected that crystal field surrounding the Tb^{3+} ions degenerate leading to change the nature of

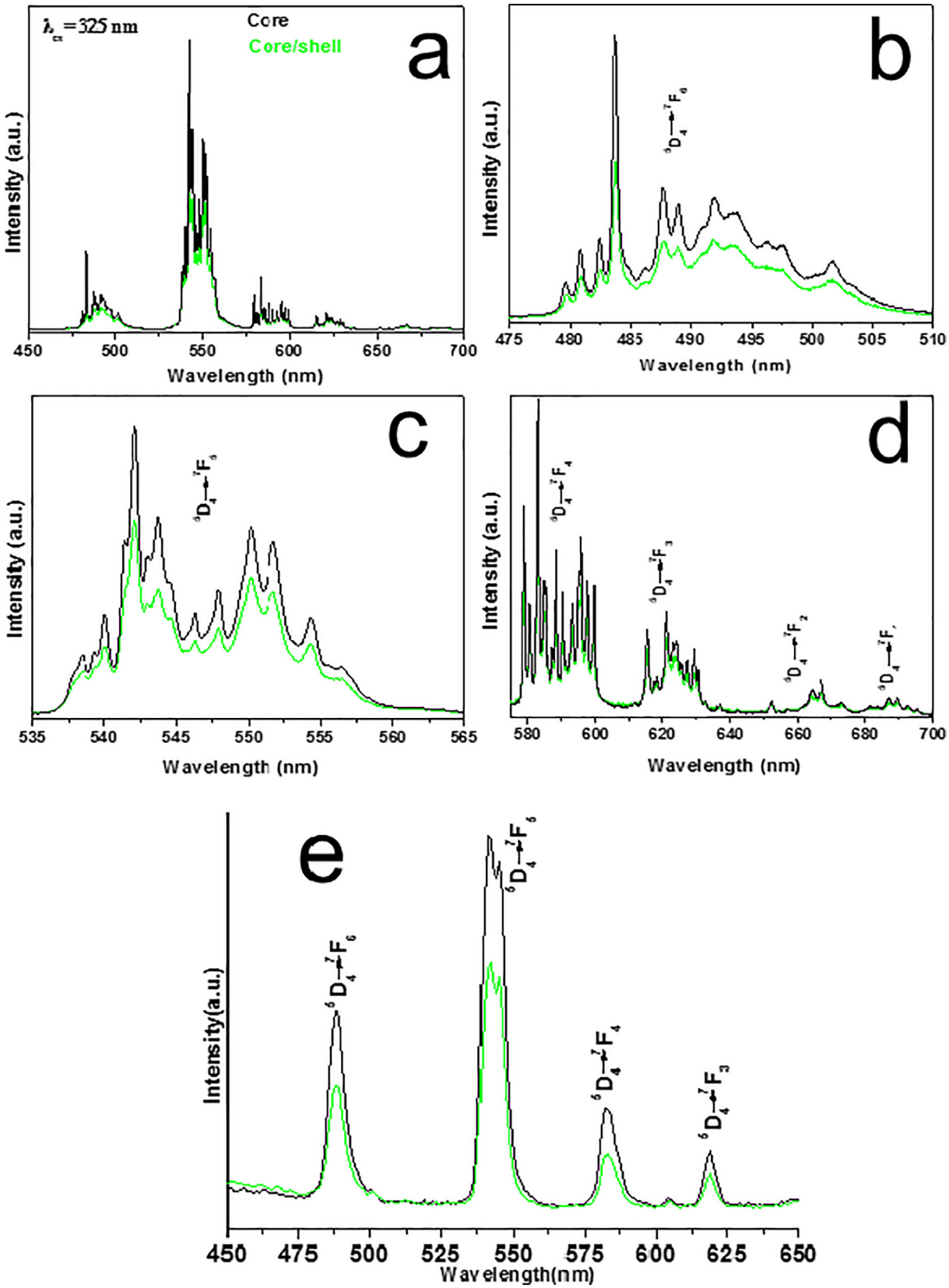

Fig. 8. Photoluminescence spectra of the core and core/shell MSs (a–d) in solid and (e) in aqueous phase.

the emission spectra of the $^5D_4 \rightarrow {}^7F_j$ compared to the other samples, and also leading to the quenching of $^5D_4 \rightarrow {}^7F_j$ overall emission intensity [47,76,77]. In general, most of the luminescent lanthanide ions revealed multiple splitting in emission transitions because of the crystal field splitting of the energy levels resulting reduced in the luminescent intensity of the emission lines [47,78–81]. It is expected that the multiple splitting in the emission transitions are related to the crystal field effect, because of the shielding effect of $5s^2p^6$ sub-shells. It is a fact that silica surface functionalization lowered the emission intensity compared to that of bare core MSs. TEM results further verified that core MSs are fully covered with an amorphous silica layer. The zeta potential values explained the surface hydrophilicity of the core/shell MSs.

4. Conclusions

In summary, highly crystalline Y_2O_3:Tb MSs with a porous surface and pure cubic phase were successfully fabricated through a thermal decomposition method at a low temperature. These luminescent core MSs were effectively encapsulated with an amorphous silica shell to form core/shell microstructures. The applied thermal decomposition method allowed slow homogeneous decomposition of a weak base (urea) for the preparation of spherical luminescent microspheres in aqueous media without any surfactants or chelating agents at low temperature. In general, this facile method may be used in the preparation of other nanoscale spherical inorganic materials. The influence of silica layer deposition on particle size, solubility, colloidal stability, surface chemistry, and luminescence properties were described and the test results for the core and core/shell MSs were also compared. The as-designed core MSs were irregular in size, spherical, and fully covered with a thick mesoporous silica layer, as confirmed from TEM micrographs. The core MSs displayed strong photoluminescence efficiency under excitation with UV radiation in the center of the visible region even after modification with a thick silica layer. However, the silica surface-modified core/shell MSs exhibited suppressed emission intensity despite their core MS counterparts owing to the presence of high-vibrational-energy surface silanol groups, which enhanced multiphoton relaxation pathways. These qualities could be highly useful towards photonic-based bio-probes because they lead to excellent dispersibility in aqueous media and the provision of important surface functional (Si—OH) groups for bio-functionalization; therefore, luminescent core/shell MSs are promising candidates for photonic-based biomedical applications.

Acknowledgement

The authors would like to extend their sincere appreciation to the Deanship of Scientific Research at King Saud University for funding this work through Research Group No. RG-1435-002.

Appendix A. Supplementary Data

Supplementary data to this article can be found online at https://doi.org/10.1016/j.saa.2018.12.015.

References

[1] Y.S. Lin, Y. Hung, H.Y. Lin, Y.H. Tseng, Y.F. Chen, C.Y. Mou, Photonic crystals from monodisperse lanthanide-hydroxide-at-silica core/shell colloidal spheres, Adv. Mater. 19 (2007) (577-+).
[2] G.A. Sotiriou, D. Franco, D. Poulikakos, A. Ferrari, Optically stable biocompatible flame-made SiO2-coated Y2O3:Tb3+ nanophosphors for cell imaging, ACS Nano 6 (2012) 3888–3897.
[3] R.C. Lv, P.P. Yang, F. He, S.L. Gai, G.X. Yang, J. Lin, Hollow structured Y2O3:Yb/Er-CuxS nanospheres with controllable size for simultaneous chemo/photothermal therapy and bioimaging, Chem. Mater. 27 (2015) 483–496.
[4] Z. Liu, Z.H. Li, J.H. Liu, S. Gu, Q.H. Yuan, J.S. Ren, X.G. Qu, Long-circulating Er3+-doped Yb2O3 up-conversion nanoparticle as an in vivo X-ray CT imaging contrast agent, Biomaterials 33 (2012) 6748–6757.
[5] Z.H. Xu, Y. Guo, T. Liu, L.M. Wang, S.S. Bian, J. Lin, General and facile method to fabricate uniform Y2O3:Ln(3+) (Ln(3+) = Eu-3+, Eu-Tb3+) hollow microspheres using polystyrene spheres as templates, J. Mater. Chem. 22 (2012) 21695–21703.
[6] G. Jia, M. Yang, Y.H. Song, H.P. You, H.J. Zhang, General and facile method to prepare uniform Y2O3:Eu hollow microspheres, Cryst. Growth Des. 9 (2009) 301–307.
[7] G. Jia, H.P. You, K. Liu, Y.H. Zheng, N. Guo, H.J. Zhang, Highly uniform Gd2O3 hollow microspheres: template-directed synthesis and luminescence properties, Langmuir 26 (2010) 5122–5128.
[8] G.A. Jia, H.P. You, Y.H. Song, Y.J. Huang, M. Yang, H.J. Zhang, Facile synthesis and luminescence of uniform Y2O3 hollow spheres by a sacrificial template route, Inorg. Chem. 49 (2010) 7721–7725.
[9] X.L. Jiang, L. Yu, C. Yao, F.Q. Zhang, J. Zhang, C.J. Li, Synthesis and characterization of Gd2O3 hollow microspheres using a template-directed method, Materials 9 (2016).
[10] H.F. Jiu, W.B. Jia, L.X. Zhang, C.S. Huang, Y.J. Feng, Q. Cheng, The synthesis and photoluminescence property of YPO4:Eu3+ hollow microspheres, Superlattice. Microst. 79 (2015) 9–14.
[11] J.G. Li, X.D. Li, X.D. Sun, T. Ishigaki, Monodispersed colloidal spheres for uniform Y2O3:Eu3+ red-phosphor particles and greatly enhanced luminescence by simultaneous Gd3+ doping, J. Phys. Chem. C 112 (2008) 11707–11716.
[12] G. Cheng, J.L. Zhang, Y.L. Liu, D.H. Sun, J.Z. Ni, Monodisperse REPO4 (RE = Yb, Gd, Y) hollow microspheres covered with nanothorns as affinity probes for selectively capturing and labeling phosphopeptides, Chem. Eur. J. 18 (2012) 2014–2020.
[13] J. Huang, Y.H. Song, Y. Sheng, K.Y. Zheng, H.B. Li, H.G. Zhang, Q.H. Huo, X.C. Xu, H.F. Zou, Gd2O2S:Eu3+ and Gd2O2S:Eu3+/Gd2O2S hollow microspheres: solvothermal preparation and luminescence properties, J. Alloys Compd. 532 (2012) 34–40.
[14] J. Huang, Y.H. Song, G.W. Wang, Y. Sheng, K.Y. Zheng, H.B. Li, H.G. Zhang, Q.S. Huo, X.C. Xu, H.F. Zou, Surfactant-assisted synthesis and luminescent properties of Gd2O3:Eu3+ core-shell microspheres, J. Alloys Compd. 574 (2013) 310–315.
[15] T. Liu, W. Xu, X. Bai, H.W. Song, Tunable silica shell and its modification on photoluminescent properties of Y2O3:Eu3+@SiO2 nanocomposites, J. Appl. Phys. 111 (2012).
[16] T.K. Pathak, H.C. Swart, R.E. Kroon, Influence of Bi doping on the structure and photoluminescence of ZnO phosphor synthesized by the combustion method, Spectrochim. Acta A 190 (2018) 164–171.
[17] F. He, P.P. Yang, D. Wang, C.X. Li, N. Niu, S.L. Gai, M.L. Zhang, Preparation and up-conversion luminescence of hollow La2O3:Ln (Ln = Yb/Er, Yb/Ho) microspheres, Langmuir 27 (2011) 5616–5623.
[18] C.C. Huang, T.Y. Liu, C.H. Su, Y.W. Lo, J.H. Chen, C.S. Yeh, Superparamagnetic hollow and paramagnetic porous Gd2O3 particles, Chem. Mater. 20 (2008) 3840–3848.
[19] Y.C. Liu, P.P. Yang, W.X. Wang, H.X. Dong, J. Lin, Fabrication and photoluminescence properties of hollow Gd2O3:Ln (Ln = Eu3+, Sm3+) spheres via a sacrificial template method, CrystEngComm 12 (2010) 3717–3723.
[20] J. Yang, Z.W. Quan, D.Y. Kong, X.M. Liu, J. Lin, Y2O3:Eu3+ microspheres: solvothermal synthesis and luminescence properties, Cryst. Growth Des. 7 (2007) 730–735.
[21] G.Y. Chen, H.C. Liu, G. Somesfalean, Y.Q. Sheng, H.J. Liang, Z.G. Zhang, Q. Sun, F.P. Wang, Enhancement of the upconversion radiation in Y2O3:Er3+ nanocrystals by codoping with Li+ ions, Appl. Phys. Lett. 92 (2008).
[22] V. Lojpur, S.P. Ahrenkiel, M.D. Dramicanin, Yb3+, Er3+ doped Y2O3 nanoparticles of different shapes prepared by self-propagating room temperature reaction method, Ceram. Int. 40 (2014) 16033–16039.
[23] G.A. Sotiriou, M. Schneider, S.E. Pratsinis, Green, silica-coated monoclinic Y2O3:Tb3+ nanophosphors: flame synthesis and characterization, J. Phys. Chem. C 116 (2012) 4493–4499.
[24] G.A. Sotiriou, M. Schneider, S.E. Pratsinis, Color-tunable nanophosphors by codoping flame-made Y2O3 with Tb and Eu, J. Phys. Chem. C 115 (2011) 1084–1089.
[25] Y.C. Wu, C. Garapon, R. Bazzi, A. Pillonnet, O. Tillement, J. Mugnier, Optical and fluorescent properties of Y2O3 sol-gel planar waveguides containing Tb3+ doped nanocrystals, Appl. Phys. A Mater. 87 (2007) 697–704.
[26] I. Cho, J.G. Kang, Y. Sohn, Photoluminescence imaging of SiO2@Y2O3:Eu(III) and SiO2@Y2O3:Tb(III) core-shell nanostructures, Bull. Kor. Chem. Soc. 35 (2014) 575–580.
[27] Q.A. Lu, Y.J. Wu, L.R. Ding, G.M. Zu, A.H. Li, Y.M. Zhao, H. Cui, Visible upconversion luminescence of Tb3+ ions in Y2O3 nanoparticles induced by a near-infrared femtosecond laser, J. Alloys Compd. 496 (2010) 488–493.
[28] M. Back, A. Massari, M. Boffelli, F. Gonella, P. Riello, D. Cristofori, R. Ricco, F. Enrichi, Optical investigation of Tb3+-doped Y2O3 nanocrystals prepared by Pechini-type sol-gel process, J. Nanopart. Res. 14 (2012).
[29] J.M. Sung, S.E. Lin, W.C.J. Wei, Synthesis and reaction kinetics for monodispersive Y2O3:Tb3+ spherical phosphor particles, J. Eur. Ceram. Soc. 27 (2007) 2605–2611.
[30] S. Ray, A. Patra, P. Pramanik, Photoluminescence properties of nanocrystalline Tb3+ doped Y2O3 phosphor prepared through a novel synthetic route, Opt. Mater. 30 (2007) 608–616.
[31] T.S. Atabaev, H.K. Kim, Y.H. Hwang, Submicron Y2O3 particles codoped with Eu and Tb ions: size controlled synthesis and tuning the luminescence emission, J. Colloid Interface Sci. 373 (2012) 14–19.
[32] S. Mukherjee, V. Sudarsan, R.K. Vatsa, S.V. Godbole, R.M. Kadam, U.M. Bhatta, A.K. Tyagi, Effect of structure, particle size and relative concentration of Eu(3+) and Tb(3+) ions on the luminescence properties of Eu(3+) co-doped Y(2)O(3):Tb nanoparticles, Nanotechnology 19 (2008).
[33] Q.Y. Meng, B.J. Chen, W. Xu, Y.M. Yang, X.X. Zhao, W.H. Di, Z. Lu, X.J. Wang, J.S. Sun, L.H. Cheng, T. Yu, Y. Peng, Size-dependent excitation spectra and energy transfer in Tb3+-doped Y2O3 nanocrystalline, J. Appl. Phys. 102 (2007).
[34] A.A. Ansari, J. Labis, A.S. Aldwayyan, M. Hezam, Facile synthesis of water-soluble luminescent mesoporous Tb(OH)(3)@SiO2 core-shell nanospheres, Nanoscale Res. Lett. 8 (2013) 1–8.

[35] A.A. Ansari, J.P. Labis, M.A. Manthrammel, Designing of luminescent GdPO4:Eu@LaPO4@SiO2 core/shell nanorods: synthesis, structural and luminescence properties, Solid State Sci. 71 (2017) 117–122.
[36] T. Grzyb, M. Runowski, K. Dabrowska, M. Giersig, S. Lis, Structural, spectroscopic and cytotoxicity studies of TbF3@CeF3 and TbF3@CeF3@SiO2 nanocrystals, J. Nanopart. Res. 15 (2013).
[37] E.J. He, H.R. Zheng, J. Dong, W. Gao, Q.Y. Han, J.N. Li, L. Hui, Y. Lu, H.N. Tian, Facile fabrication and upconversion luminescence enhancement of LaF3:Yb3+/Ln(3+)@SiO2 (Ln = Er, Tm) nanostructures decorated with Ag nanoparticles, Nanotechnology 25 (2014).
[38] W.W. Hu, Q.S. Chen, H.H. Li, Q. Ouyang, J.W. Zhao, Fabricating a novel label-free aptasensor for acetamiprid by fluorescence resonance energy transfer between NH2-NaYF4: Yb, Ho@SiO2 and Au nanoparticles, Biosens. Bioelectron. 80 (2016) 398–404.
[39] C. Kai, G. Chao, P. Bo, W. Wei, The influence of SiO2 shell on fluorescent properties of LaF3:Nd3+/SiO2 core/shell nanoparticles, J. Nanomater. (2010), 238792. 1-5.
[40] X.J. Kang, Z.Y. Cheng, C.X. Li, D.M. Yang, M.M. Shang, P.A. Ma, G.G. Li, N.A. Liu, J. Lin, Core-shell structured up-conversion luminescent and mesoporous NaYF4:Yb3+/Er3+@nSiO(2)@mSiO(2) nanospheres as carriers for drug delivery, J. Phys. Chem. C 115 (2011) 15801–15811.
[41] U. Kostiv, V. Patsula, A. Noculak, A. Podhorodecki, D. Vetvicka, P. Pouckova, Z. Sedlakova, D. Horak, Phthalocyanine-conjugated upconversion NaYF4:Yb3+/Er3+@SiO2 nanospheres for NIR-triggered photodynamic therapy in a tumor mouse model, ChemMedChem 12 (2017) 2066–2073.
[42] L.L. Liang, Y.M. Liu, C.H. Bu, K.M. Guo, W.W. Sun, N. Huang, T. Peng, B. Sebo, M.M. Pan, W. Liu, S.S. Guo, X.Z. Zhao, Highly uniform, bifunctional core/double-shell-structured-NaYF4:Er3+, Yb3+@SiO2@TiO2 hexagonal sub-microprisms for high-performance dye sensitized solar cells, Adv. Mater. 25 (2013) 2174–2180.
[43] L.L. Liang, Y.M. Liu, X.Z. Zhao, Double-shell beta-NaYF4:Yb3+, Er3+/SiO2/TiO2 submicroplates as a scattering and upconverting layer for efficient dye-sensitized solar cells, Chem. Commun. 49 (2013) 3958–3960.
[44] Y.X. Fu, Y.H. Sun, Comparative study of synthesis and characterization of monodispersed SiO2@Y2O3:Eu3+ and SiO2@Y2O3:Eu3+@SiO2 core-shell structure phosphor particles, J. Alloys Compd. 471 (2009) 190–196.
[45] A.A. Ansari, M. Alam, J.P. Labis, S.A. Alrokayan, G. Shafi, T.N. Hasan, N.A. Syed, A.A. Alshatwi, Luminescent mesoporous LaVO4:Eu3+ core-shell nanoparticles: synthesis, characterization, biocompatibility and their cytotoxicity, J. Mater. Chem. 21 (2011) 19310–19316.
[46] A.A. Ansari, T.N. Hasan, N.A. Syed, J.P. Labis, A.K. Parchur, G. Shafi, A.A. Alshatwi, In-vitro cyto-toxicity, geno-toxicity, and bio-imaging evaluation of one-pot synthesized luminescent functionalized mesoporous SiO2@Eu(OH)(3) core-shell microspheres, Nanomed. Nanotechnol. 9 (2013) 1328–1335.
[47] A.A. Ansari, J.P. Labis, One-pot synthesis and photoluminescence properties of luminescent functionalized mesoporous SiO2@Tb(OH)(3) core-shell nanospheres, J. Mater. Chem. 22 (2012) 16649–16656.
[48] A.A. Ansari, A. Khan, J.P. Labis, M. Alam, M. Aslam Manthrammel, M. Ahamed, M.J. Akhtar, A. Aldalbahi, H. Ghaithan, Mesoporous multi-silica layer-coated Y2O3:Eu core-shell nanoparticles: synthesis, luminescent properties and cytotoxicity evaluation, Mater. Sci. Eng. C 96 (2019) 365–373.
[49] R.C. Lv, S.L. Gai, Y.L. Dai, F. He, N. Niu, P.P. Yang, Surfactant-free synthesis, luminescent properties, and drug-release properties of LaF3 and LaCO3F hollow microspheres, Inorg. Chem. 53 (2014) 998–1008.
[50] P.P. Yang, S.L. Gai, Y.C. Liu, W.X. Wang, C.X. Li, J. Lin, Uniform hollow Lu2O3:Ln (Ln = Eu3+, Tb3+) spheres: facile synthesis and luminescent properties, Inorg. Chem. 50 (2011) 2182–2190.
[51] A.A. Ansari, A.K. Parchur, M. Alam, A. Azzeer, Structural and photoluminescence properties of Tb-doped CaMoO4 nanoparticles with sequential surface coatings, Mater. Chem. Phys. 147 (2014) 715–721.
[52] A.A. Ansari, R. Yadav, S.B. Rai, Enhanced luminescence efficiency of aqueous dispersible NaYF4:Yb/Er nanoparticles and the effect of surface coating, RSC Adv. 6 (2016) 22074–22082.
[53] A.A. Ansari, A.K. Parchur, M. Alam, J. Labis, A. Azzeer, Influence of surface coating on structural and photoluminescent properties of CaMoO4:Pr nanoparticles, J. Fluoresc. 24 (2014) 1253–1262.
[54] A.A. Ansari, J. Labis, M. Alam, S.M. Ramay, N. Ahmad, A. Mahmood, Effect of cobalt doping on structural, optical and redox properties cerium oxide nanoparticles, Phase Transit. 89 (2016) 261–272.
[55] Q. Lu, F.Y. Guo, L. Sun, A.H. Li, L.C. Zhao, Silica-/titania-coated Y(2)O(3):Tm(3+), Yb(3+) nanoparticles with improvement in upconversion luminescence induced by different thickness shells, J. Appl. Phys. 103 (2008).
[56] J.P. Yang, Y.H. Deng, Q.L. Wu, J. Zhou, H.F. Bao, Q. Li, F. Zhang, F.Y. Li, B. Tu, D.Y. Zhao, Mesoporous silica encapsulating upconversion luminescence rare-earth fluoride nanorods for secondary excitation, Langmuir 26 (2010) 8850–8856.
[57] X.F. Qiao, J.C. Zhou, J.W. Xiao, Y.F. Wang, L.D. Sun, C.H. Yan, Triple-functional core-shell structured upconversion luminescent nanoparticles covalently grafted with photosensitizer for luminescent, magnetic resonance imaging and photodynamic therapy in vitro, Nanoscale 4 (2012) 4611–4623.
[58] H. Wang, C.K. Lin, X.M. Liu, J. Lin, M. Yu, Monodisperse spherical core-shell-structured phosphors obtained by functionalization of silica spheres with Y2O3:Eu3+ layers for field emission displays, Appl. Phys. Lett. 87 (2005).
[59] M. Yu, J. Lin, J. Fang, Silica spheres coated with YVO4:Eu3+ layers via sol-gel process: a simple method to obtain spherical core-shell phosphors, Chem. Mater. 17 (2005) 1783–1791.
[60] A.A. Ansari, A. Aldalbahi, J.P. Labis, A.M. El-Toni, M. Ahamed, M.A. Manthrammel, Highly biocompatible, monodispersed and mesoporous La(OH)(3):Eu@mSiO(2) core-shell nanospheres: synthesis and luminescent properties, Colloids Surf. B 163 (2018) 133–139.
[61] M. Runowski, T. Grzyb, A. Zep, P. Krzyczkowska, E. Gorecka, M. Giersig, S. Lis, Eu3+ and Tb3+ doped LaPO4 nanorods, modified with a luminescent organic compound, exhibiting tunable multicolour emission, RSC Adv. 4 (2014) 46305–46312.
[62] M. Runowski, S. Goderski, J. Paczesny, M. Ksiezopolska-Gocalska, A. Ekner-Grzyb, T. Grzyb, J.D. Rybka, M. Giersig, S. Lis, Preparation of biocompatible, luminescent-plasmonic core/shell nanomaterials based on lanthanide and gold nanoparticles exhibiting SERS effects, J. Phys. Chem. C 120 (2016) 23788–23798.
[63] A.A. Ansari, Silica-modified luminescent LaPO4:Eu@LaPO4@SiO2 core/shell nanorods: Synthesis, structural and luminescent properties, Luminescence 33 (2018) 112–118.
[64] A.A. Ansari, S.P. Singh, N. Singh, B.D. Malhotra, Synthesis of optically active silica-coated NdF3 core-shell nanoparticles, Spectrochim. Acta A 86 (2012) 432–436.
[65] A.A. Ansari, A.K. Parchur, B. Kumar, S.B. Rai, Highly aqueous soluble CaF2:Ce/Tb nanocrystals: effect of surface functionalization on structural, optical band gap, and photoluminescence properties, J. Mater. Sci. Mater. Med. 27 (2016).
[66] M. Yu, H. Wang, C.K. Lin, G.Z. Li, J. Lin, Sol-gel synthesis and photoluminescence properties of spherical SiO2@LaPO4:Ce3+/Tb3+ particles with a core-shell structure, Nanotechnology 17 (2006) 3245–3252.
[67] Z.H. Xu, C.X. Li, P.A. Ma, Z.Y. Hou, D.M. Yang, X.J. Kang, J. Lin, Facile synthesis of an up-conversion luminescent and mesoporous Gd2O3:Er3+@nSiO(2)@mSiO(2) nanocomposite as a drug carrier, Nanoscale 3 (2011) 661–667.
[68] M. He, P. Huang, C. Zhang, J. Ma, R. He, D. Cui, Phase- and size-controllable synthesis of hexagonal upconversion rare-earth fluoride nanocrystals through an oleic acid/ionic liquid two-phase system, Chem. Eur. J. 18 (2012) 5954–5969.
[69] Q. Lue, A.H. Li, F.Y. Guo, L. Sun, L.C. Zhao, The two-photon excitation of SiO(2)-coated Y(2)O(3):Eu(3+) nanoparticles by a near-infrared femtosecond laser, Nanotechnology 19 (2008).
[70] H. Guo, Y.M. Qiao, Preparation, characterization, and strong upconversion of monodisperse Y2O3:Er3+, Yb3+ microspheres, Opt. Mater. 31 (2009) 583–589.
[71] A.A. Ansari, N. Singh, A.F. Khan, S.P. Singh, K. Iftikhar, Solvent effect on optical properties of hydrated lanthanide tris-acetylacetone, J. Lumin. 127 (2007) 446–452.
[72] C.X. Li, Z.Y. Hou, Y.L. Dai, D.M. Yang, Z.Y. Cheng, P.A. Ma, J. Lin, A facile fabrication of upconversion luminescent and mesoporous core-shell structured beta-NaYF4:Yb3+, Er3+@mSiO(2) nanocomposite spheres for anti-cancer drug delivery and cell imaging, Biomater. Sci. 1 (2013) 213–223.
[73] Z.Y. Hou, C.X. Li, P.A. Ma, Z.Y. Cheng, X.J. Li, X. Zhang, Y.L. Dai, D.M. Yang, H.Z. Lian, J. Lin, Up-conversion luminescent and porous NaYF4:Yb3+, Er3+@SiO2 nanocomposite fibers for anti-cancer drug delivery and cell imaging, Adv. Funct. Mater. 22 (2012) 2713–2722.
[74] R.S. Loitongbam, W.R. Singh, G. Phaomei, N.S. Singh, Blue and green emission from Ce3+ and Tb3+ co-doped Y2O3 nanoparticles, J. Lumin. 140 (2013) 95–102.
[75] A.K. Parchur, A.I. Prasad, A.A. Ansari, S.B. Rai, R.S. Ningthoujam, Luminescence properties of Tb3+-doped CaMoO4 nanoparticles: annealing effect, polar medium dispersible, polymer film and core-shell formation, Dalton Trans. 41 (2012) 11032–11045.
[76] Y. Wang, X. Bai, T. Liu, B.A. Dong, L. Xu, Q.O. Liu, H.W. Song, Solvothermal synthesis and luminescence properties of monodisperse Gd2O3:Eu3+ and Gd2O3:Eu3+@SiO2 nanospheres, J. Solid State Chem. 183 (2010) 2779–2785.
[77] E.M. Goldys, K. Drozdowicz-Tomsia, J.J. Sun, D. Dosev, I.M. Kennedy, S. Yatsunenko, M. Godlewski, Optical characterization of Eu-doped and undoped Gd2O3 nanoparticles synthesized by the hydrogen flame pyrolysis method, J. Am. Chem. Soc. 128 (2006) 14498–14505.
[78] S. Chandra, F.L. Deepak, J.B. Gruber, D.K. Sardar, Synthesis, morphology, and optical characterization of nanocrystalline Er3+:Y2O3, J. Phys. Chem. C 114 (2010) 874–880.
[79] W.H. Di, M.G. Willinger, R.A.S. Ferreira, X.G. Ren, S.Z. Lu, N. Pinna, Citric acid-assisted hydrothermal synthesis of luminescent TbPO(4):Eu nanocrystals: controlled morphology and tunable emission, J. Phys. Chem. C 112 (2008) 18815–18820.
[80] J.W. Stouwdam, G.A. Hebbink, J. Huskens, F.C.J.M. van Veggel, Lanthanide-doped nanoparticles with excellent luminescent properties in organic media, Chem. Mater. 15 (2003) 4604–4616.
[81] K. Riwotzki, H. Meyssamy, A. Kornowski, M. Haase, Liquid-phase synthesis of doped nanoparticles: colloids of luminescing LaPO4:Eu and CePO4:Tb particles with a narrow particle size distribution, J. Phys. Chem. B 104 (2000) 2824–2828.